

Catalysis of a Protein Folding Reaction: Mechanistic Implications of the 2.0 Å Structure of the Subtilisin–Prodomain Complex^{†,‡}

Philip Bryan,* Lan Wang, Joel Hoskins, Sergei Ruvinov, Susan Strausberg, Patrick Alexander, Orna Almog, Gary Gilliland, and Travis Gallagher

Center for Advanced Research in Biotechnology, University of Maryland Biotechnology Institute, 9600 Gudelsky Drive, Rockville, Maryland 20850

Received April 17, 1995; Revised Manuscript Received June 7, 1995[§]

ABSTRACT: Biosynthesis of subtilisin is dependent on a 77 amino acid, N-terminal prodomain, which is autocatalytically processed to create the mature form of the enzyme [Ikemura, H., Takagi, H., & Inouye, M. (1987) *J. Biol. Chem.* 262, 7859–7864]. In order to better understand the role of the prodomain in subtilisin folding, we have determined the structure of the processed complex between the prodomain and subtilisin Sbt-70, a mutant engineered for facilitated folding. The prodomain is largely unstructured by itself but folds into a compact structure with a four-stranded antiparallel β -sheet and two three-turn α -helices when complexed with subtilisin. The K_a of the complex is $2 \times 10^8 \text{ M}^{-1}$ at 25 °C. The prodomain binds on subtilisin's two parallel surface α -helices and supplies caps to the N-termini of the two helices. The C-terminal strand of the prodomain binds in the subtilisin substrate binding cleft. While Sbt-70 is capable of independent folding, the prodomain accelerates the process by a factor of $>10^7 \text{ M}^{-1}$ of prodomain in 30 mM Tris-HCl, pH 7.5, at 25 °C. X-ray structures of the mutant subtilisin folded *in vitro* either with or without the prodomain are compared and show that the identical folded state is achieved in either case. A model of the folding reaction of Sbt-70 and the prodomain is described as the following equilibria: $P + S_u \leftrightarrow P_f-S_i \leftrightarrow P_f-S_f$, where S_u and P are Sbt-70 and prodomain, respectively, which are largely unstructured at the start of the reaction, P_f-S_i is a collision complex of a partially folded Sbt-70 and folded prodomain, and P_f-S_f is the complex of folded Sbt-70 and prodomain. The mode of prodomain binding suggests that it catalyzes subtilisin folding by stabilizing the central $\alpha\beta\alpha$ substructure in subtilisin. The prodomain bound to this substructure may correspond to the collision complex, P_f-S_i , whose formation is rate limiting in the bimolecular reaction [Strausberg, S., Alexander, P., Wang, L., Schwarz, F., & Bryan, P. (1993) *Biochemistry* 32, 8112–8119].

The folding of many proteins is a thermodynamically determined process which spontaneously occurs *in vitro* under favorable conditions (Kim & Baldwin, 1990). The kinetic barrier separating the folded and unfolded forms of such proteins is surprisingly small considering the problem presented by finding the native conformation among the large number of nonnative ones (Levinthal, 1968). The apparent formidability of the entropy problem led to the suggestion that proteins fold by following an energetic pathway of increasingly structured intermediates which leads to the native state rather than sampling from among denatured states of approximately equal energy until falling into a free energy well when the native conformation happens to be encountered (Creighton, 1992).

The 275 amino acid serine protease subtilisin, as well as several other extracellular microbial proteases, are unusual but not unique examples of proteins for which the native state is difficult to access from the unfolded state (Baker & Agard, 1994). The biosynthesis of subtilisin is dependent on a 77 amino acid, N-terminal activation domain, which is autocatalytically processed to create the mature form of the enzyme (Ikemura et al., 1987). Secreted proteases are

usually synthesized as inactive proenzymes which are then processed following secretion into the active form. This maturation process may be biologically imperative to delay protease activation and protect intracellular proteins. As a result, the biological folding unit which evolved is the proprotease rather than the mature protease. Some secreted proteases, such as trypsin, are capable of facile folding in mature form (Higaki et al., 1989). For subtilisin, the proenzyme has a facility for folding which the stable, mature enzyme lacks, suggesting that a folding pathway is not a necessary consequence of a stable native state but rather an additional constraint on protein evolution.

Mature subtilisin, once denatured, refolds to the native state very slowly ($\tau > \text{weeks}$) in the absence of the prodomain (Bryan et al., 1992). Even when catalyzed by the isolated prodomain in a bimolecular reaction, refolding of subtilisin occurs at a rate of only $\sim 0.2 \text{ s}^{-1} \text{ M}^{-1}$ of prodomain (Eder et al., 1993a). The slow time scale of *in vitro* folding makes thermodynamic and kinetic analysis of the process problematic. To make the study of subtilisin folding more tractable, we have mutated subtilisin to accelerate the folding reaction. A major part of the kinetic barrier to folding subtilisin involves formation of a high-affinity calcium binding site ($K_a = 10^7 \text{ M}^{-1}$ at 25 °C), called site A (Bryan et al., 1992). Deletion of amino acids 75–83 removes the calcium A-site and destabilizes subtilisin but greatly accelerates both uncatalyzed folding and prodomain-catalyzed folding (Straus-

[†] This work was supported by NIH Grant GM42560.

[‡] The coordinates have been deposited in the Brookhaven Protein Data Bank (file name 1SPB).

* Corresponding author.

[§] Abstract published in *Advance ACS Abstracts*, July 15, 1995.

berg et al., 1993b). The subtilisin mutant used in these studies is denoted Sbt-70¹ and contains the following mutations: $\Delta 75-83$ (to eliminate calcium binding and accelerate the folding rate); S221A² (to remove the active site nucleophile and eliminate proteolytic activity); and K43N, M50F, A73L, Q206V, Y217K, and N218S (to restore stability lost due to the calcium loop deletion) (Strausberg et al., 1995). None of these mutant amino acids except A221 contact the prodomain in the bimolecular complex.

While Sbt-70 is capable of independent folding, the prodomain accelerates the process by a factor of $>10^7$ M⁻¹ of prodomain in 30 mM Tris-HCl, pH 7.5, at 25 °C. The K_a of the resulting complex is 2×10^8 (Strausberg et al., 1993b). This paper suggests a mechanism by which the prodomain accelerates folding based on analyses of the 2.0 Å resolution structure of the folded complex and the kinetics of catalyzed folding.

MATERIALS AND METHODS

Engineering Subtilisin for Facile Folding. The subtilisin used in this study was an engineered version which lacks the high-affinity calcium site A. Calcium is an integral part of the subtilisin structure, and deletion of the calcium binding loop (residues 75–83) decreases its conformational stability. To recover the lost stability, the mutations (K43N, M50F, A73L, Q206V, Y217K, and N218S) were introduced into $\Delta 75-83$ subtilisin. These mutations cumulatively increase the half-life of thermal inactivation at 55 °C by ~ 100 -fold relative to $\Delta 75-83$ subtilisin. This mutant, denoted Sbt-67, has native-like catalytic activity against the synthetic substrate sAAPF-pNA (specific activity of 160 units/mg, compared with 85 units/mg for wild-type subtilisin BPN'). Subtilisin with calcium-independent stability is of biotechnological interest and details of its engineering are described in Strausberg et al. (1995).

To prevent autodegradation from occurring during the unfolding and refolding, a catalytically impaired subtilisin was constructed by mutating the active-site serine 221 of Sbt-67 to alanine. This mutation has little effect on the stability of subtilisin but reduces peptidase activity by a factor of 10^6 (Carter & Wells, 1988). The resulting mutant is denoted Sbt-70.

Mutagenesis of the cloned subtilisin gene from *Bacillus amyloliquefaciens* (subtilisin BPN') was performed according to the oligonucleotide-directed *in vitro* mutagenesis system, version 2 (Amersham International plc). Single-strand plasmid DNA was sequenced according to Sequenase (United States Biochemical).

Expression and Purification of the Cloned Prodomain. The propeptide region of the subtilisin BPN' gene was

subcloned using the polymerase chain reaction as described (Strausberg et al., 1993b). The *Escherichia coli* production strain was grown at 37 °C in a 1.5 L BioFlo Model fermenter until an $OD_{600} = 1-1.5$ was attained at which time 1 mM IPTG was added to induce the production of T7 RNA polymerase that directs transcription of the target DNA. Two hours after induction the cells were harvested. *E. coli* paste from a 1.5 L fermentation (5 g) was suspended in 50 mL of cold phosphate buffered saline (PBS), and PMSF was added to a final concentration of 1 mM. DNase I (1 mg) in 2 mL of 40 mM Tris-HCl and 1 M MgCl₂ was also added. This suspension was heated to 80 °C for 5 min. After the reaction was cooled on ice, another addition of PMSF and DNase I was made. This mixture was centrifuged at 25000g for 30 min.

The soluble, heat-released protein was dialyzed extensively against 20 mM HEPES, pH 7.0, and purified to homogeneity by anion exchange chromatography with DE52 followed by cation exchange chromatography using SE53. Five grams of *E. coli* paste yields 30–60 mg of purified propeptide. The strategy is analogous to that described in detail for high-level production of the 56 amino acid protein G, B-domain (Alexander et al., 1992a). Prodomain concentration [P] was determined using $[P]^{0.1\%} = 0.67$ at 275 nm (Strausberg, et al., 1993b).

Cloning of Mature Sbt-70 Subtilisin in *E. coli*. A unique *Nde*I site was inserted before codon 1 of the mature region of the Sbt-70 subtilisin gene using the mutagenic oligonucleotide GCA CAT GCG TAC CAT ATG GCG CAG TCC G, thus allowing a precise fusion to the ATG initiation codon of the expression plasmid (pG5), which is a modified version of pT7-7 (Alexander et al., 1992a). The coding region of the mature portion of the gene was excised as a *Nde*I–*Sal*I fragment and ligated into pG5. This results in a precise fusion of the subtilisin gene with the expression signals of the plasmid. The resulting plasmid was designated pJ12. The N-terminal methionine synthesized in the *E. coli* production system appears to be removed by posttranslational processing and was absent in the final product.

Expression and Purification of Mature Sbt-70 in *E. coli*. One liter of Luria–Bertani medium containing 100 μ g/mL ampicillin was inoculated with 10 mL of a fresh overnight culture of pJ12 in *E. coli* BL21DE3 and grown at 37 °C, 250 rpm in 2 L baffled flasks to $OD_{600} = 1.0$. IPTG was added to 1 mM and the culture grown an additional 3 h at 37 °C, 250 rpm to $OD_{600} = 1.8$. Cells were recovered by centrifugation and stored at –70 °C prior to purification.

Induced cells (9.7 g) were resuspended in 50 mL of 50 mM Tris, pH 8.0/100 mM NaCl/1 mM EDTA, and PMSF was added to 1 mM. The cells were lysed by French Press and 125 μ L of DNase I (10 mg/mL) were added and allowed to incubate at room temperature for 15 min. Inclusion bodies containing Sbt-70 were recovered by centrifugation at 10000g, 4 °C, for 20 min. The resulting pellet was washed three times by repeated resuspension in 60 mL of ice-cold 20 mM Hepes, pH 7.0, and centrifugation at 10000g, 4 °C, for 10 min. The final pellet was resuspended in 50 mL of ice-cold 20 mM Hepes, pH 7.0, containing 2 M urea, frozen on dry ice and allowed to thaw at RT. The solution was centrifuged at 10000g, 4 °C, for 10 min and the supernatant applied to a Productiv DE cartridge (Metachem Technologies Inc., P/N 4300) equilibrated with 20 mM Hepes, pH 7.0/2 M urea. The cartridge was washed with 40 mL of cold 20

¹ Abbreviations: CD, circular dichroism; $\Delta 75-83$ subtilisin, subtilisin BPN' with a deletion of amino acids 75–83; cps, counts per second; EDTA, disodium salt of ethylenediaminetetraacetic acid; HEPES, *N*-(2-hydroxyethyl)piperazine-*N'*-2-ethanesulfonic acid; IPTG, isopropyl β -D-thiogalactopyranoside; K_a , association constant for propeptide binding; OD_{600} , optical density at 600 nm; [P], propeptide concentration; P_i, phosphate; [S], subtilisin concentration; sAAPF-pNA, succinyl-L-Ala-L-Ala-L-Pro-L-Phe-p-nitroanilide; Sbt-70, subtilisin BPN' with the following mutations: K43N, M50F, A73L, $\Delta 75-83$, Q206V, Y217K, N218S, and S221A; Tris, tris(hydroxymethyl)aminomethane; τ = reciprocal of the rate constant for folding.

² A shorthand for denoting amino acid substitutions employs the single-letter amino acid code as follows: Y217K denotes the change of Tyr 217 to Lys.

mM Hepes, pH 7.0/2 M urea. Flow through and wash fractions of Sbt-70 were combined and renatured by overnight dialysis at 25 °C against 3.5 L of 0.1 M KPi , pH 7.0. The rate of folding of Sbt-70, as well as other $\Delta 75$ –83 subtilisins, is slow ($<0.00005 \text{ s}^{-1}$) in 20 mM Hepes, pH 7.0, but increases as ionic strength is raised (Bryan et al., 1992). In 0.1 M KPi , pH 7.0, the folding rate of Sbt-70 is 0.001 s^{-1} .

A-L-A-L Affinity Chromatography. An affinity agarose column was prepared by coupling the tetrapeptide A-L-A-L (Sigma, P/N A-3546) to Affi-Gel 10 (Bio-Rad, P/N 153-6099) following the manufacturer's protocol. The DE cartridge-purified and renatured Sbt-70 was split and each half loaded onto a 4.5 mL column of A-L-A-L-agarose equilibrated with 20 mM Hepes, pH 7.0. The column was washed with 20 mL of 20 mM Hepes, pH 7.0/1 M NaCl followed by 10 mL of 20 mM Hepes, pH 7.0, and Sbt-70 was eluted with 50 mM triethylamine/ H_2O , pH 11.1. One milliliter peak fractions of Sbt-70 were immediately neutralized by the addition of 0.1 mL of 0.1 M potassium phosphate, pH 7.0, combined, and dialyzed overnight against 3.5 L of 2 mM ammonium bicarbonate, pH 7.0. Purified Sbt-70 (60 mg) was lyophilized and stored at -20°C .

Protein purity was checked by sodium dodecyl sulfate (SDS)–polyacrylamide gel electrophoresis (Novex). Assays of peptidase activity were performed by monitoring the hydrolysis of sAAPF-pNA as described (DelMar et al., 1979). Sbt-70 concentration $[S]$ was determined using $[S]^{0.1\%} = 1.12$ at 280 nm (Pantoliano et al., 1989).

Crystallization of Sbt-70 and Data Collection. The best crystals were obtained by hanging drop vapor diffusion method. The crystallization drops were prepared by mixing 5 mL of Sbt-70 solution (12 mg/mL protein in a solution of 10 mM Hepes/HCl, pH 7.0, 50 mM NaCl) with an equal volume of 1.25 M Li_2SO_4 and 0.1 M HEPES/HCl, pH 7.5. These drops were then suspended over a 1 mL reservoir of 1.25 M Li_2SO_4 and 0.1 M HEPES/HCl, pH 7.5. Well-shaped crystals could be observed in the drop (usually 1–4 crystals) after about 3 days. Within another 2 weeks these crystals usually grew to their full size, $0.3 \times 0.3 \times 0.5 \text{ mm}$. The crystals were in the space group $P2_12_12_1$ with cell constants $a = 60.67 \text{ \AA}$, $b = 84.02 \text{ \AA}$, and $c = 54.17 \text{ \AA}$.

The X-ray data were collected at room temperature with a Siemens/Xentronics area detector mounted on a Rigaku generator and were processed using Xengen (Howard et al., 1987). These data consisted of a total of 11081 unique reflections [$I > 2.0\sigma(I)$] with an R_{merge} of 9.8%, which represent 78% of the data to 2.2 \AA . The structure was solved by molecular replacement technique using the Amore program and S15 subtilisin (PDB entry, 1suc) as a model.

Crystallization and data collection for the prodomain–subtilisin complex will be described in Gallagher, Gilliland, Wang, and Bryan (*Structure*, in press).

Spectroscopy. Circular dichroism (CD) measurements were performed with a Jasco 720 spectropolarimeter using a water-jacketed cell. Temperature control was provided by a Neslab RTE-110 circulating water bath interfaced with a MTP-6 temperature programmer.

Unfolding and refolding reactions were followed by monitoring change in tryptophan fluorescence (excitation $\lambda = 300 \text{ nm}$, emission $\lambda = 345 \text{ nm}$) using a SPEX FluoroMax spectrofluorimeter for manual mixing experiments and a

KinTek Stopped-Flow Model SF2001 for rapid kinetic measurements as described (Strausberg et al., 1993b).

RESULTS

Structural Comparison of Sbt-70 Folded with and without the Prodomain. To help establish the catalytic role of the prodomain in subtilisin folding, we wished to demonstrate that the prodomain directs subtilisin to the identical state as is achieved in the uncatalyzed reaction. Skepticism has persisted regarding whether $\Delta 75$ –83 subtilisin can refold to the native state without the prodomain (Eder et al., 1993a; Shinde & Inouye, 1993a), despite previous demonstrations of apparent reversibility based on CD and fluorescence spectroscopy (Bryan et al., 1992; Strausberg et al., 1993a). Two alternative interpretations of our data have been suggested: (1) that $\Delta 75$ –83 subtilisin is not completely unfolded by our denaturation procedures and that a core of residual structure allows refolding to the native state to occur (Shinde et al., 1993b); (2) that $\Delta 75$ –83 subtilisin does not actually refold to the native state but to a native-like molten globular state (Eder et al., 1993a).

To address these interpretations, high-resolution structures of subtilisins folded *in vitro* either with or without the prodomain were determined by X-ray diffraction and compared. The region of the Sbt-70 subtilisin gene encoding only the mature portion of subtilisin was cloned from *Bacillus* into an inducible *E. coli* expression system such that the synthesis of mature subtilisin was driven by the phage T7 promoter as described in Materials and Methods. The 266 amino acid Sbt-70 protein was expressed at high levels (30% of total cellular protein) in *E. coli*. The Sbt-70 was recovered from inclusion bodies and resolubilized in urea. In one case the mutant subtilisin was folded by dialysis against 0.1 M KPi , pH 7.0, at 25 °C without the prodomain as described in Materials and Methods. In the other case, 25 μM mutant subtilisin was folded by dialysis against 0.1 M KPi , pH 7.0, at 25 °C with 25 μM purified prodomain. The purified, *in vitro* folded subtilisin and subtilisin–prodomain complex were crystallized and structures determined to 2.2 and 2.0 \AA resolution, respectively. The refined structures are superimposable with an RMS deviation of 0.46 \AA between 264 α -carbon atoms.

In vitro folded Sbt-70 superimposed with wild-type subtilisin produced in *B. subtilis* through the normal, prodomain-mediated, biosynthetic pathway with an RMS deviation of 0.49 between 264 α -carbon atoms. This experiment demonstrates that $\Delta 75$ –83 subtilisin, synthesized in a foreign host and never in contact with the prodomain, folds to the native state.

Characterization of the Trapped, Denatured State. Subtilisin denatured under various conditions has been examined by circular dichroism. Sbt-70 is denatured by 25 mM HCl (pH 1.85) within several seconds. The far-UV CD spectrum is shown in Figure 1A. If Sbt-70 is returned to native conditions by quickly raising the pH to 7.5 by the addition of 30 mM Tris base, little change in the CD spectrum is observed after 1 h at 25 °C. This can be seen by comparing the circular dichroism spectrum of Sbt-70 at pH 1.85 to the spectrum of the same solution neutralized to pH 7.5 (Figure 1A). The spectra are very similar and indicate structures with considerable disorder compared to the native state. The rates of independent folding of $\Delta 75$ –83 subtilisins have been

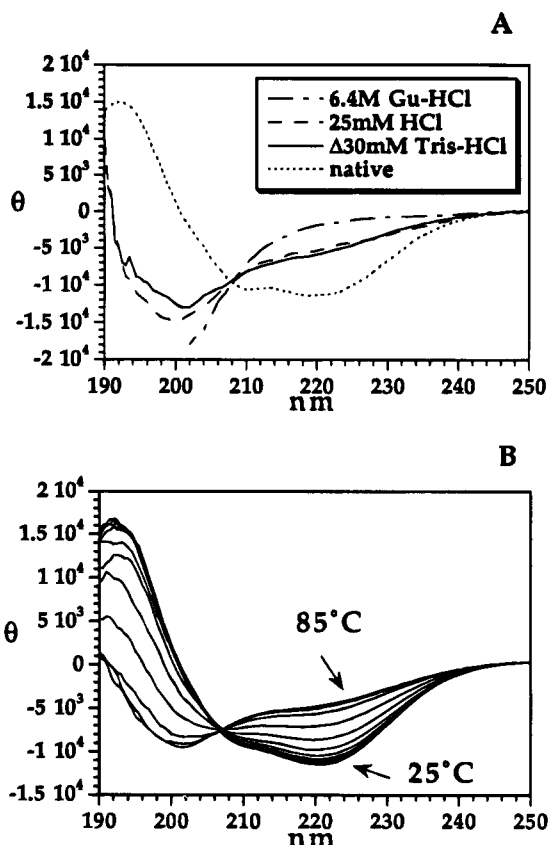


FIGURE 1: Circular dichroism of Sbt-70. Mean residue ellipticity ($\text{deg cm}^2/\text{dmol}$) is plotted versus wavelength. (A) Far-UV CD spectra of Sbt-70 denatured under various conditions and the spectrum of the native protein are shown. Spectra were measured using a 1 mm cylindrical cuvette with $[\text{Sbt-70}] = 3.7 \mu\text{M}$. (B) Far-UV CD spectra of Sbt-70 as a function of temperature. Scans taken at 5 °C intervals from 25 to 85 °C are shown. Spectra were measured using a 0.1 mm cylindrical cuvette with $[\text{Sbt-70}] = 37 \mu\text{M}$ in 50 mM glycine, pH 9.0.

shown previously to be ionic strength dependent (Bryan et al., 1992; Strausberg et al., 1993a). At low ionic strength (e.g., 30 mM Tris-HCl, pH 7.5) the native state of Sbt-70 is stable but the rate of folding is slow ($<0.00005 \text{ s}^{-1}$). We will refer to denatured Sbt-70 in 30 mM Tris-HCl, pH 7.5, as the trapped, denatured state.

The disorder in the trapped, denatured state was assessed by comparing its CD spectrum with that of Gu-HCl (6.4 M) denatured Sbt-70 (Figure 1A). The trapped state appears to have more regular secondary structure than Gu-HCl denatured protein, whose spectrum is closer to that of a random coil. The trapped state is easily accessible from the Gu-HCl denatured state. If Gu-HCl denatured Sbt-70 is diluted into native conditions (30 mM Tris-HCl, pH 7.5, 0.064 M Gu-HCl), it collapses within a second to a structure with spectral properties similar to the trapped state induced after acid denaturation. After the initial burst phase following dilution from Gu-HCl, the rate of folding is independent of which denaturant is used to induce unfolding.

The amount of secondary structure in the trapped, denatured state is similar to the heat-denatured state (Figure 1B). Heating the trapped, denatured state to 85 °C induces no further loss of secondary structure. The heat denatured state of subtilisin is fairly typical of the globular proteins such as lysozyme and staphylococcal nuclease (Kuwajima et al., 1985; Sugawara et al., 1991). The heat capacity increase

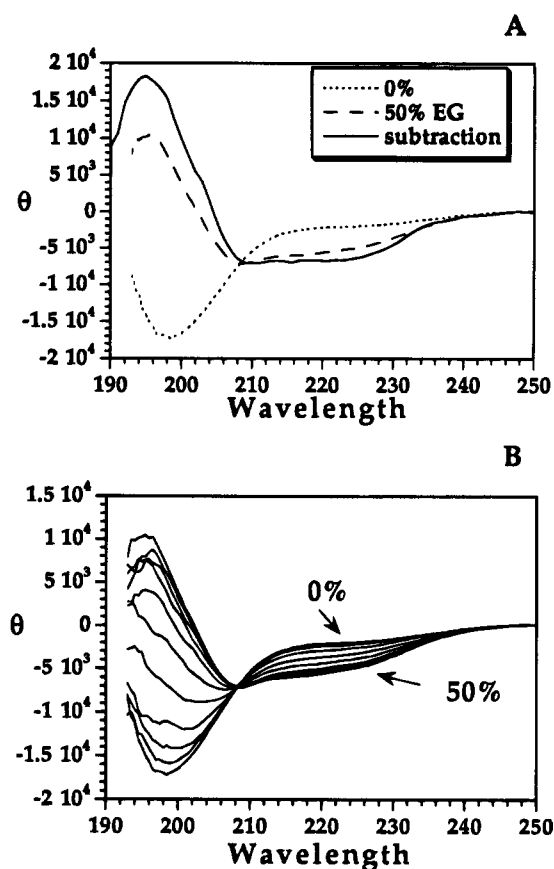


FIGURE 2: Circular dichroism of the prodomain. Mean residue ellipticity ($\text{deg cm}^2/\text{dmol}$) is plotted versus wavelength. (A) CD spectrum of the isolated prodomain, difference spectrum ($100 \mu\text{M}$ prodomain-subtilisin complex minus $100 \mu\text{M}$ subtilisin), and CD spectrum of the isolated prodomain in 50% EG are shown. Spectra were measured in 0.1 M KPi , pH 7.0, using a 0.1 mm cylindrical cuvette at 25 °C. (B) Far-UV CD spectra of prodomain in 0.1 M P_i , pH 7.0, plus ethylene glycol are shown. Spectra were taken at ~4% intervals from 0–50% EG using a 0.05 mm cylindrical cuvette with $[\text{P}] = 300 \mu\text{M}$.

upon thermal denaturation is large ($\sim 4 \text{ kcal/deg mol}$) as expected for a protein of its size and indicates a high degree of hydration in the heat denatured form (Pantoliano et al., 1989).

Trapped, denatured Sbt-70 appears by CD to be more disordered than the compact denatured (molten globule) state observed for α -lactalbumin at pH 2.0 (Kuwajima et al., 1985). The denatured form of Sbt-70 trapped in 30 mM Tris-HCl, pH 7.5, appears to be kinetically isolated from its native form and from highly structured intermediates.

Structure and Stability of the Isolated Prodomain. The prodomain, which is largely unstructured by itself, folds into a compact structure with a four stranded antiparallel β -sheet and two three-turn α -helices when complexed with Sbt-70. Figure 2A shows the CD spectrum of the isolated prodomain, which is typical of a largely random coil structure with a minimum ellipticity at 198 nm. Since no changes in the native subtilisin structure are induced by prodomain binding, the difference spectrum of the complex minus subtilisin corresponds to the CD spectrum of the bound prodomain (Strausberg et al., 1993b). The subtracted spectrum is as expected for a protein with the α -helical and β -sheet content observed in the X-ray structure (Figure 2A).

Because of its ability to catalyze folding, we suspected that the prodomain had a propensity to fold on its own, even

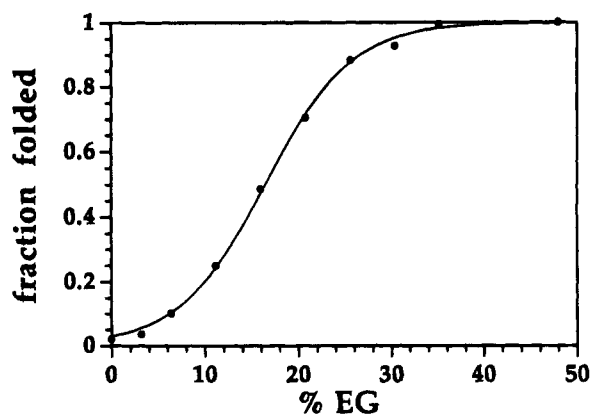
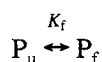


FIGURE 3: Apparent fraction of prodomain folded vs [EG]. Fraction of folded protein was calculated from the CD signal at 220 nm as described in the text. Prodomain was in 0.1 M KPi , pH 7.0.

though the equilibrium constant for independent folding obviously favors the unfolded state. We used the stabilizing agent ethylene glycol (EG) to induce folded structure in the isolated prodomain (Timasheff, 1993). Above 40% EG, CD spectra of the prodomain resemble its spectrum in complex with subtilisin. The subtracted spectrum of the prodomain in complex with subtilisin is compared with the spectrum induced by 50% EG in Figure 2A. The two spectra, while similar, are not identical probably due the influences of subtilisin on the prodomain which cannot be mimicked by EG, such as the binding of the C-terminal part of the prodomain in the substrate binding cleft of subtilisin (see below). A folding profile was produced by measuring the amount of prodomain structure as a function of ethylene glycol concentration (Figure 2B). The folding transition has a clear isodichroic point consistent with a two state equilibrium. The apparent fraction folded was calculated from the ellipticity at 220 nm, and the data were fit to the equation for a two state equilibrium (Figure 3):

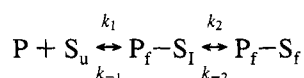


The apparent equilibrium constant, K_f , was calculated from

$$\text{fraction folded} = 1/[1 + \exp(m_1 - m_2x)]$$

where $m_1 = -\ln K_f$, $m_2 = \Delta(-\ln K_f)/\Delta\%EG$, and $x = \%EG$ (Pace et al., 1990). K_f for independent folding extrapolates to 0.03 at 0% ethylene glycol, corresponding to $\Delta G_{\text{folding}} = \sim 2$ kcal/mol at 25 °C. The free energy of independent folding of the prodomain, although unfavorable, is small enough that a few percent of prodomain molecules appear to be folded under aqueous conditions at 20 °C.

Kinetics of prodomain-catalyzed Sbt-70 folding. The prodomain-catalyzed folding of Sbt-70 can be modeled as the following equilibria:



where P is prodomain, which is largely unstructured at the start of the reaction; S_u is unfolded subtilisin; P_f-S_I is a collision complex of a partially-folded subtilisin intermediate and folded prodomain; P_f-S_f is the complex of folded subtilisin and folded prodomain (Strausberg et al., 1993b).

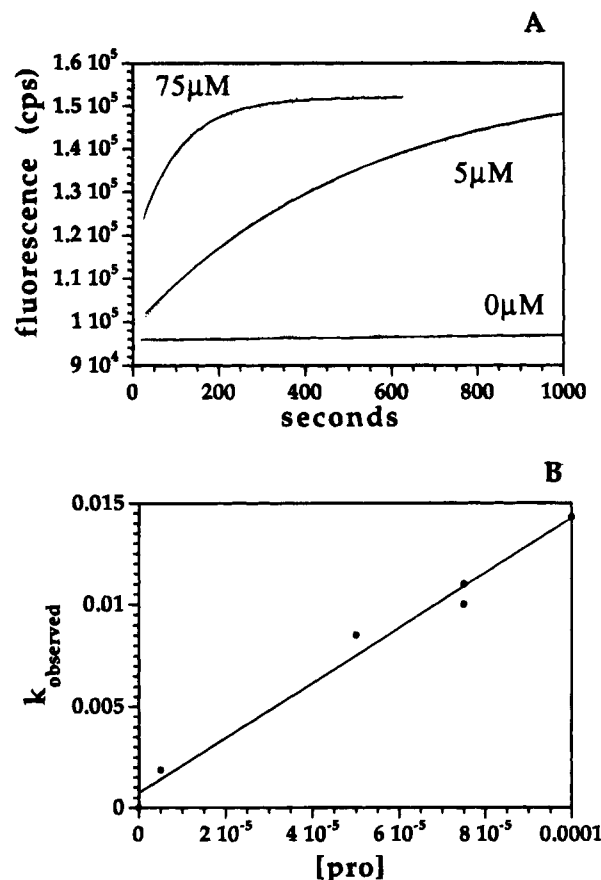


FIGURE 4: Kinetics of prodomain-catalyzed folding. (A) Denatured Sbt-70 (1 μM) and various concentrations of prodomain were mixed in 5 mM KPi and 30 mM Tris, pH 7.5, at 25 °C. The final prodomain concentrations are indicated on the graph. After manual mixing, the reaction was followed by the increase in tryptophan fluorescence which occurs upon folding of subtilisin into the prodomain-subtilisin complex. The curves plotted are the average of three experiments at each [P]. The data are fit to a single-exponential equation to determine a pseudo-first-order rate constant for folding (solid lines). (B) The pseudo-first-order rate constant for folding, k_{observed} , is plotted as a function of [P].

The folding reaction of subtilisin, in the presence of prodomain, can be followed by an increase in tryptophan fluorescence of 1.7-fold due to changes in the environments of the three tryptophans in subtilisin upon its folding and binding of the prodomain. The prodomain does not contain tryptophan residues and thus has no intrinsic fluorescence at 345 nm if an excitation wavelength of 300 nm is used. Therefore, fluorescence increases observed at 345 nm are due solely to the conversion of S_u to P_f-S_f .

As described above, denatured Sbt-70 when returned to native conditions at low ionic strength is kinetically isolated from the native state. In 30 mM Tris and 5 mM KPi , pH 7.5, the rate of uncatalyzed folding of Sbt-70 is $< 5 \times 10^{-5} \text{ s}^{-1}$ at 25 °C (Figure 4A). When the isolated and largely unstructured prodomain is added, the rate of subtilisin folding increases with the concentration of prodomain, [P]. The folding reaction was followed using $[S_u] = 1 \mu\text{M}$ and varying [P] from 5 to 100 μM . Under conditions of excess [P], the experiments measure a single cycle of subtilisin folding and obey first-order kinetics. The folding curves were fit with a single-exponential equation to determine k_{observed} for each [P] (Figure 4A). The k_{observed} plotted as a function of [P] is linear up to [P] = 100 μM (Figure 4B). The absence of curvature in this plot implies that the isomerization of P_f-S_f

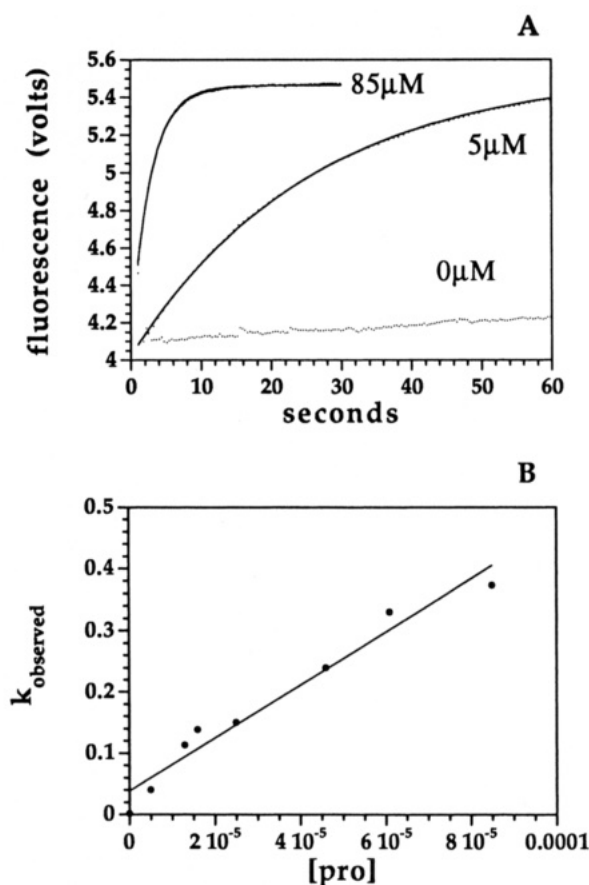


FIGURE 5: Kinetics of prodomain-catalyzed folding with ethylene glycol. (A) Denatured Sbt-70 (1 μM) and various concentrations of prodomain were mixed in 5 mM KP_i and 30 mM Tris, pH 7.5, + 40% EG at 25 $^{\circ}\text{C}$. The final prodomain concentrations are indicated on the graph. After stopped-flow mixing, the reaction was followed by the increase in tryptophan fluorescence. The curves plotted are the average of 10–12 experiments at each $[P]$. The data are fit to a single-exponential equation to determine a pseudo-first-order rate constant for folding (solid lines). (B) The pseudo-first-order rate constant for folding, k_{observed} , is plotted as a function of $[P]$.

S_I to P_I – S_I is rapid relative to its formation (Strausberg et al., 1993b). Over the range of $[P]$ examined here the formation of a productive collision complex, P_I – S_I , appears to be the limiting step in the reaction. The slope of k_{observed} vs $[P]$ is equal to a second-order rate constant for catalyzed subtilisin folding of $150 \text{ M}^{-1} \text{ s}^{-1}$. The overall rate acceleration under these conditions $>10^7 \text{ M}^{-1}$ of prodomain.

Rate of Catalyzed Folding in Ethylene Glycol. If the folded prodomain is the productive form in catalyzing subtilisin folding and the folded form of the prodomain is stabilized by ethylene glycol, then it follows that the rate of catalyzed folding may be increased by ethylene glycol. Sbt-70 was denatured in 25 mM HCl and renatured in 30 mM Tris and 5 mM KP_i , pH 7.5, + 40% ethylene glycol. The uncatalyzed rate of Sbt-70 folding is 0.0018 s^{-1} under these conditions. The folding reaction was followed using $[S_0] = 1 \text{ } \mu\text{M}$ and varying $[P]$ from 5 to $100 \text{ } \mu\text{M}$. The rate of Sbt-70 folding is accelerated with increasing $[P]$, and, as seen without EG, the reaction is a pseudo-first-order kinetic process (Figure 5A). A plot of k_{observed} vs $[P]$ yields a second-order rate constant for catalyzed subtilisin folding in 40% EG of $4500 \text{ M}^{-1} \text{ s}^{-1}$, about 30 times faster than the rate without EG (Figure 5B). This increased rate is consistent with the increased independent stability of the prodomain

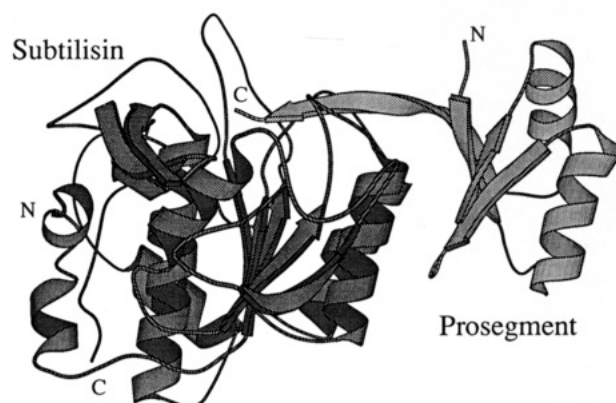


FIGURE 6: Prodomain–subtilisin complex. Ribbon drawing depicting the α -carbon backbone of the bimolecular complex of $\Delta 75$ –83 subtilisin (darker shading) and the prodomain (lighter shading). The C-terminus of the prodomain is in the subtilisin active site.

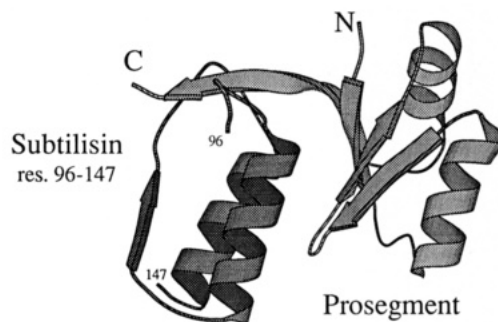


FIGURE 7: Prodomain interactions with the $\alpha\beta\alpha$ substructure in subtilisin. Ribbon drawing depicting the α -carbon backbone of the prodomain (lighter shading) and its binding site on subtilisin (darker shading). Almost all of the prodomain's contacts with subtilisin are made with residues 100–144. It is proposed that the prodomain accelerates folding by stabilizing this $\alpha\beta\alpha$ substructure in the subtilisin folding reaction.

in 40% EG. The increase in the rate of uncatalyzed Sbt-70 folding in EG indicates, however, that partially folded intermediates of Sbt-70 also are stabilized independently of prodomain binding. The combination of these effects appears to result in a significant stabilization of the intermediate, P_I – S_I , relative to other unfolded states and hence a significant acceleration of catalyzed folding in EG.

Structure of the Prodomain–Subtilisin Complex. In the complex, the prodomain folds into a single compact domain with an antiparallel four-stranded β -sheet and two three-turn α -helices (Figure 6). The K_a of the complex is $2 \times 10^8 \text{ M}^{-1}$ at 25 $^{\circ}\text{C}$ (Strausberg et al., 1993b). The β -sheet of the prodomain packs tightly against the two parallel surface α -helices of subtilisin (residues 104–116 and 133–144) as shown in Figure 7. Pro residues E69 and D71 form helix caps for the N-termini of the two subtilisin helices. In another charge dipole interaction, the carboxylate of E112 of subtilisin accepts hydrogen bonds from the peptide nitrogens of Pro residues 42, 43, and 44 (Figure 8).

The C-terminal residues 72–77 extend out from the central part of the prodomain and bind in a substrate-like manner along subtilisin's active site cleft. Residues Y77, A76, H75, and A74 of the prodomain occupy subsites S1–S4 of subtilisin, respectively. Almost all of the prodomain's contacts with subtilisin are made with residues 100–144.

The simplest model of catalyzed folding is one in which the observed binding interaction in the complex accelerates folding by stabilizing the 45 amino acid $\alpha\beta\alpha$ substructure

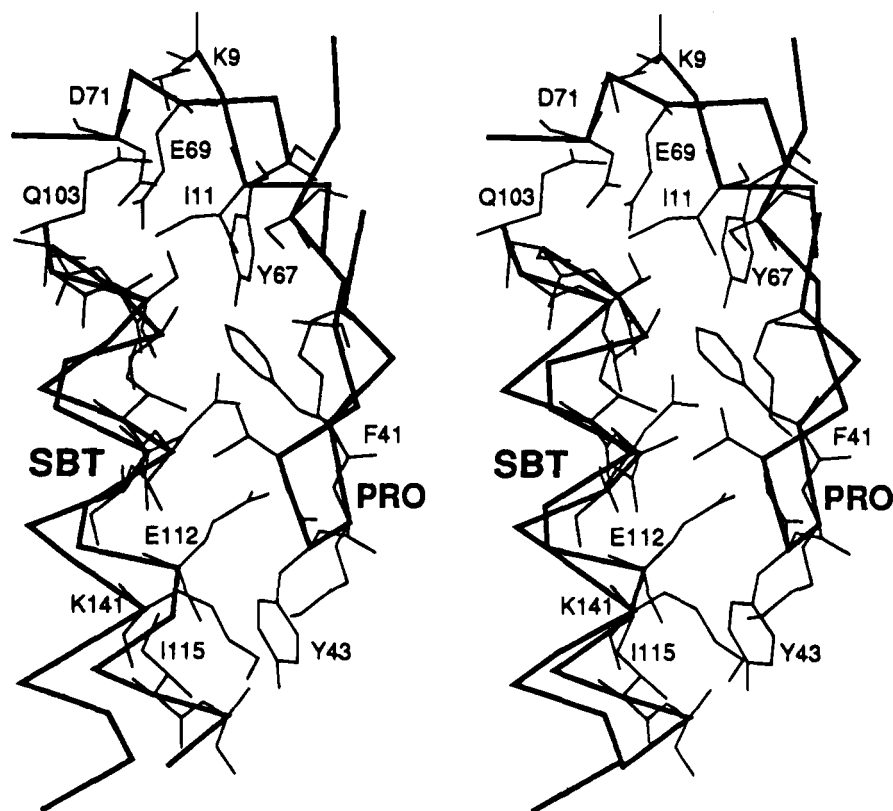


FIGURE 8: Subtilisin–prodomain interface. Stereoview of the binding interface between the two surface α -helices of subtilisin and the β -sheet of the prodomain. Residues pictured but unlabeled for subtilisin are S105, I108, N109, A116, S132, A133, A134, A137, and A138. Residues pictured but unlabeled for the prodomain are K39, K42, K44, A46, and S48. Note the prodomain's helix capping residues D71 and E69 and subtilisin's β -bend capping residue E112. F41 is the central residue of the prodomain which forms the hydrophobic interface with the two surface α -helices of subtilisin.

in subtilisin (Figure 7). Once the $\alpha\beta\alpha$ substructure forms, it may act as a folding nucleus with subsequent folding propagating into N and C-terminal regions of subtilisin. The acceleration of subtilisin folding is not simply a function of tight binding of the prodomain in the subtilisin substrate binding cleft. Tight-binding subtilisin inhibitors SSI and eglin have no effect on the rate of subtilisin folding. These inhibitors bind subtilisins with association constants of 10^{10} – 10^{12} M $^{-1}$ (Laskowski & Kato, 1980), exclusively through substrate-like interactions with the subtilisin binding cleft (McPhalen & James, 1988; Takeuchi et al., 1991). The prodomain appears to function rather by binding to the $\alpha\beta\alpha$ structure whose formation appears to be rate limiting in folding.

DISCUSSION

The Role of the Prodomain in Trans-Catalyzed Folding. Denatured Sbt-70, when returned to native conditions at low ionic strength, remains largely disordered and kinetically isolated from the native state, even though the native form is the global thermodynamic minimum. CD spectra suggest that the unfolded state of Sbt-70 under native conditions (30 mM Tris, pH 7.5), while not completely random, is a heterogeneous collection of relatively unfolded conformations.

Kinetic isolation of the folded state from partially folded intermediates could be a property of particular importance for a broad specificity protease, such as subtilisin, since intermediates in dynamic equilibrium with active subtilisin would rapidly be proteolyzed. The consequence of high cooperativity under native conditions is that there is no

efficient pathway to reach the native state because partially folded intermediate states have low stabilities. An efficient folding pathway implies that productive intermediates are significantly more stable than the surrounding landscape of unfolded and misfolded conformations. The slow folding of Sbt-70 supports the argument that proteins require a pathway of stable intermediates in order to fold efficiently. In subtilisin, native (productive) intermediates appear to have similar or lower stability than unfolded or misfolded states. This may result in a large entropic barrier to folding since the entire native structure may have to be formed before a significant free energy well is reached in conformational space.

On the basis of the structure of the bimolecular complex between Sbt-70 and the prodomain, we propose that the prodomain facilitates folding by stabilizing the central $\alpha\beta\alpha$ substructure in subtilisin. The prodomain binds on subtilisin's two parallel surface α -helices and supplies caps to the N-termini of the two helices. The prodomain may stabilize this productive intermediate relative to other unfolded states. In the absence of the prodomain, the $\alpha\beta\alpha$ substructure does not have sufficient independent stability to initiate folding very frequently. The prodomain bound to this substructure may correspond to the collision complex, P_F-S_I , whose formation is rate limiting in the bimolecular reaction. Subsequent folding may propagate from this folding nucleus into N- and C-terminal regions of subtilisin.

If the prodomain were a stable structure independent of subtilisin, then it would be easier to understand how it could catalyze folding by binding to and stabilizing a native-like

transition state. The folded prodomain is a compact structure with shape complementarity and high affinity to native subtilisin. The low independent stability of the prodomain, however, decreases the binding energy that it can contribute to stabilizing a transition state because the cost of folding the prodomain must be paid for with its binding energy.

How much independent stability must an intermediate have in order to propagate folding? Let us consider the prodomain and Sbt-70 together comprising a single folding unit. Sbt-70 alone appears to lack intermediates of sufficient stability for efficient folding. The equilibrium constant for independent folding of the prodomain is tilted toward unfolding such that only a few percent of the population are folded at 25 °C. The stability of the prodomain nevertheless is sufficient for it to provide a nucleus for subtilisin folding. The bimolecular folding of the prodomain and Sbt-70 is probably not entirely different from the situation of a monomeric folding unit since the stabilities of intermediates are low for monomeric proteins with two-state folding behavior.

Bimolecular vs Unimolecular Folding. The manner in which the prodomain binds to subtilisin supports a unimolecular model for subtilisin maturation *in vivo*. The C-terminus of the prodomain binds in the active site cleft of subtilisin in a substrate-like manner with Y77 occupying the S1 subsite of subtilisin. The *in vivo* process would involve folding, self-cleavage, and repositioning of the mature N-terminus away from the active site to its native position. In wild-type subtilisin this involves coordination of calcium because the N-terminus (Gln 2) supplies one ligand to calcium at the high-affinity A-site. If we assume prosubtilisin folds unimolecularly to produce the observed interdomain contact, then it follows that processing is unimolecular. Otherwise the interface would have to dissolve in order to make the Y77 available to a second active site. The N-terminus of mature subtilisin can be modeled in an active site conformer by minor torsional reorganizations involving residues 1–10. In this conformer, residues Ala 1 and Gln 2 occupy the S1' and S2' substrate sites. According to this model, the calcium A-site cannot be fully formed until after the cleavage step because Gln 2 cannot simultaneously bind in the S2' subsite and bind to calcium in the A-site. Thus the covalent attachment of the propeptide to subtilisin would prevent the final folding of the calcium A-site region, until after cleavage to produce the mature enzyme. A requirement of covalent attachment of the propeptide to subtilisin for proper formation of the calcium A-site is consistent with the fact that both bimolecular, catalyzed folding and uncatalyzed folding of $\Delta 75-83$ subtilisin are much more rapid than for subtilisin with the natural calcium A-site.

Apart from a specific role in the formation of the A-site, tethering the prodomain to mature subtilisin would be expected to increase the local concentration of the prodomain and make its collisions with subtilisin more frequent. The local concentration of the prodomain relative to its $\alpha\beta\alpha$ binding site would be on the order of 10 μM (assuming a tether of 100 amino acids in extended conformation).³ Although we and others (Eder et al., 1993b) have synthesized unprocessed prosubtilisin, measurements of the kinetics of

folding are not easily interpretable because of the uncertainty as to what the folded state of prosubtilisin is. Unprocessed prosubtilisin is metastable and may have the following schizophrenic behavior: If the N-terminal amino acids of mature subtilisin are in their final native position bound to calcium at the A-site, then the prodomain will be dislocated from its binding surface on subtilisin. On the other hand if prosubtilisin is an active site conformer with the N-terminus bound in the substrate binding site, then it cannot occupy its final native position in the A-site.⁴

Conclusions. The proform of subtilisin has a facility for folding which the stable, mature enzyme lacks. This appears to be an example in which an efficient folding pathway is not a necessary consequence of a stable native state. The difficulty in folding the mature protease may be due to a lack of partially folded intermediates of sufficient stability to propagate folding and supports the argument that proteins require a pathway of stable intermediates in order to fold efficiently. The prodomain appears to provide this missing element by acting as an early folding nucleus. The structure of the prodomain–subtilisin complex suggests that the prodomain binds and stabilizes the $\alpha\beta\alpha$ substructure of subtilisin, whose formation is rate limiting in the bimolecular folding reaction described here.

ACKNOWLEDGMENT

We thank John Moult, Jan Pederson, Edward Eisenstein, David Baker, and David Shortle for helpful discussion and Masatsune Kainosho for a generous gift of *Streptomyces subtilisin* inhibitor. The identification of commercial equipment and materials in this paper does not imply recommendation or endorsement by the National Institute of Standards and Technology.

REFERENCES

- Alexander, P., Fahnestock, S., Lee, T., Orban, J., & Bryan, P. (1992a) *Biochemistry* 31, 3597–3603.
- Alexander, P., Orban, J., & Bryan, P. (1992b) *Biochemistry* 31, 7243–7248.
- Baker, D., & Agard, D. (1994) *Biochemistry* 33, 7505–7509.
- Bryan, P., Alexander, P., Strausberg, S., Schwarz, F., Wang, L., Gilliland, G., & Gallagher, D. T. (1992) *Biochemistry* 31, 4937–4945.
- Carter, P., & Wells, J. A. (1988) *Nature* 332, 564–568.
- Creighton, T. E. (1992) *Protein Folding*, Freeman, New York.
- DelMar, E., Largman, C., Brodrick, J., & Geokas, M. (1979) *Anal. Biochem.* 99, 316–320.
- Eder, J., Rheinhecker, M., & Fersht, A. R. (1993a) *Biochemistry* 32, 18–26.
- Eder, J., Rheinhecker, M., & Fersht, A. R. (1993b) *J. Mol. Biol.* 233, 293–304.
- Gallagher, T. D., Gilliland, G., Wang, L., & Bryan, P. (1995) *Structure* (in press).
- Higaki, J. N., Evnin, L. B., & Craik, C. S. (1989) *Biochemistry* 28, 9256–9263.
- Howard, A. J., Gilliland, G. L., Finzel, B. C., Poulos, T. L., Ohlendorf, D. H., & Salemme, F. R. (1987) *J. Appl. Crystallogr.* 20, 383–387.

³ A local concentration of $\sim 10 \mu\text{M}$ is calculated by assuming the maximum distance that the prodomain and the $\alpha\beta\alpha$ substructure can be separated in unprocessed prosubtilisin is 100 amino acids in extended conformation (360 Å). The concentration of one molecule in a sphere of radius 360 Å equals 8.5 μM .

⁴ Unprocessed prosubtilisin has been crystallized in our laboratory, but the crystals obtained to date diffract poorly.

- Ikemura, H., Takagi, H., & Inouye, M. (1987) *J. Biol. Chem.* 262, 7859–7864.
- Kim, P. S., & Baldwin, R. L. (1990) *Annu. Rev. Biochem.* 59, 631–660.
- Kuwajima, K., Hiraoka, Y., Ikeguchi, M., & Sugai, S. (1985) *Biochemistry* 24, 874–881.
- Laskowski, M., & Kato, I. (1980) *Annu. Rev. Biochem.* 49, 593–626.
- Levinthal, C. (1968) *J. Chim. Phys.* 65, 44–45.
- McPhalen, C. A., & James, M. N. G. (1988) *Biochemistry* 27, 6582–6598.
- Orban, J., Alexander, P., & Bryan, P. (1994) *Biochemistry* 33, 5702–5710.
- Pace, C. N., Laurents, D. V., & Thomson, J. A. (1990) 29, 2564–2572.
- Pantoliano, M. W., Whitlow, M., Wood, J. F., Dodd, S. W., Hardman, K. D., Rollence, M. L., & Bryan, P. N. (1989) *Biochemistry* 28, 7205–7213.
- Shinde, U., & Inouye, M. (1993) *Trends Biochem. Sci.* 18, 442–446.
- Shinde, U., Li, Y., Chatterjee, S., & Inouye, M. (1993) *Proc. Natl. Acad. Sci. U.S.A.* 90, 6924–6928.
- Strausberg, S., Alexander, P., Wang, L., Gallagher, D. T., Gilliland, G., & Bryan, P. (1993a) *Biochemistry* 32, 10371–10377.
- Strausberg, S., Alexander, P., Wang, L., Schwarz, F., & Bryan, P. (1993b) *Biochemistry* 32, 8112–8119.
- Strausberg, S., Alexander, P., Gallagher, D. T., Gilliland, G., Barnett, B. L., & Bryan, P. (1995) *Bio/technology* 13, 669–673.
- Sugawara, T., Kuwajima, K., & Sugai, S. (1991) *Biochemistry* 30, 2698–2706.
- Takeuchi, Y., Satow, Y., Nakamura, K. T., & Mitsui, Y. (1991) *J. Mol. Biol.* 221, 309–325.
- Timasheff, S. N. (1993) *Annu. Rev. Biophys. Biomol. Struct.* 22, 67–97.

BI950862Q

Corrections

Views of Helical Peptides: A Proposal for the Position of 3_{10} -Helix along the Thermodynamic Folding Pathway, by Glenn L. Millhauser, Volume 34, Number 12, March 28, 1995, pages 3873–3877.

Page 3874. The abscissa of Figure 1, labeled as the total fraction of helix, represents the fraction of peptide chains that contain at least one hydrogen bond. However, in the last paragraph of the first column on page 3874, the abscissa was referred to as the fractional helicity. This use of fractional helicity is incorrect since this phrase is usually reversed, in Zimm–Bragg theory, to indicate the number of helical hydrogen bonds formed divided by the maximum number of hydrogen bonds possible in the fully helical state (N_h). Recalculation of components represented in Figure 1 against the proper definition of fractional helicity indicates that the population of peptides containing short helical domains reaches a maximum at a fractional helicity of 0.20. At 0.50 fractional helicity, short domains comprise approximately 12% of the peptide chains containing helix (but only 3% of the hydrogen bonds). While the result of this illustrative calculation is rendered somewhat less emphatic, the conclusions from the calculation and the rest of the paper remain unchanged and support the proposal of 3_{10} -helix as a thermodynamic folding intermediate. Prof. A. Holtzer is gratefully acknowledged for identifying this issue and for many helpful suggestions.

BI955007L